Future Journal of Pharmaceutical Sciences

RESEARCH

Open Access

Molecular docking, antimicrobial, antibiofilm formation, and antiproliferative activities of furano-based sesquiterpenoids from *Euryops arabicus*

Fayza A. Aljohany[1], Samyah D. Jastaniah[2], Fatima B. Alamri[3], Nahed O. Bawakid[1], Hanan I. Althagbi[4], Ashraf B. Abdel-Naim[5], Mohammad Y. Alfaifi[6], Magda M. Aly[2,7], Fitri Budiyanto[8] and Walied M. Alarif[9*]

Abstract

Background *Euryops arabicus* is well known in the Arabian Peninsula as traditional herbal medicine. The plant synthesizes various types of flavonoids, terpenes, and furoermophilanes skeletons in either steroidal or nonsteroidal conformation, and this wide range of chemical compounds might play an increasingly prominent role in medicine. This study aimed to isolate pure secondary metabolites and assess their antibacterial, antiproliferation, and antibiofilm formation properties.

Methods The organic extract of the areal parts of *E. arabicus* was chromatographically fractionated to afford pure compounds characterized using NMR, UV, and IR along with mass spectrometry. The activity of the isolated compounds was assessed against three cancer cells and a set of Gram-negative and positive bacteria.

Results Four specific sesquiterpenoids were identified: 6β-senecioyloxy-1,10-dehydrofuranoeremophilan-9-one (**1**), 6β-acetoxy-9-oxoeuryopsin (**2**), 6β-(2′-methyl, 2′,3′-epoxy-butyryloxy)-euryopsin (**3**), and 6β-angloyloxy-1,10-dehydrofuraoeremophilan-9-one (**4**). Molecular docking studies indicated the epidermal growth factor receptor and methionyl-tRNA synthetase as probable antibacterial and antiproliferative activities of the compounds. In the in vitro studies, compounds **2** and **4** showed remarkable activity against all examined Gram-negative and positive pathogens with inhibition diameters (mm) ranging from 13.1 ± 0.23 to 19.0 ± 0.44 and 12.9 ± 0.20 to 16.2 ± 0.23, respectively. Compounds **2** and **4** showed moderate biofilm formation inhibition of both *Pseudomonas aeruginosa* and *Staphylococcus aureus* with 58% and 79%, respectively. Moreover, the isolated sesquiterpenoids showed potent antiproliferative activities against MCF-7, HepG2, and HCT116 human cancer cells.

Conclusion Four sesquiterpenoids were isolated from *E. arabicus*. Compound **2** showed a relatively high antibacterial and cytotoxic activity. Additional studies are recommended to substantiate the observed activities further.

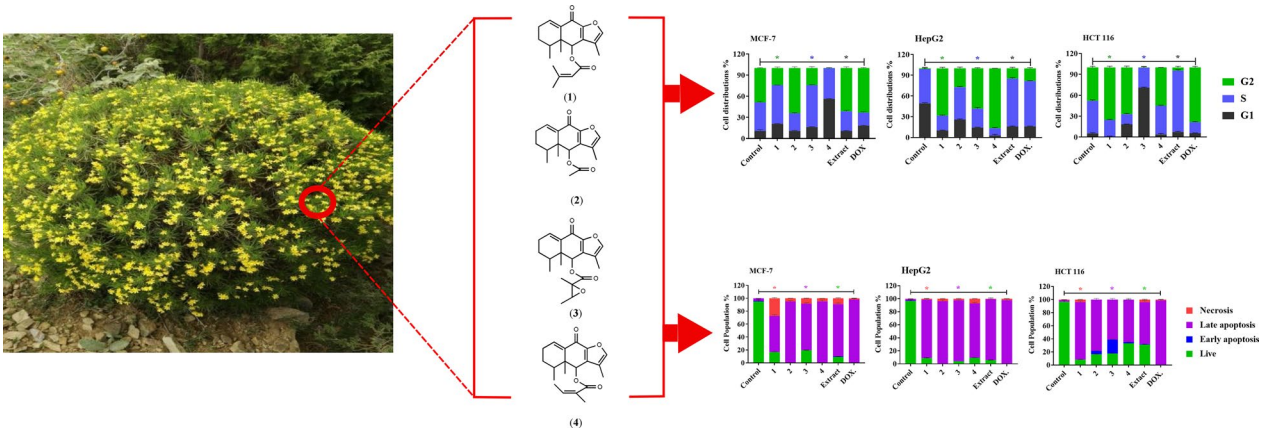
Keywords Asteraceae, Sesquiterpenes, Antibacterial, Apoptosis, Cell cycle analysis

*Correspondence:
Walied M. Alarif
welaref@kau.edu.sa
Full list of author information is available at the end of the article

Springer Open

© The Author(s) 2025. **Open Access** This article is licensed under a Creative Commons Attribution 4.0 International License, which permits use, sharing, adaptation, distribution and reproduction in any medium or format, as long as you give appropriate credit to the original author(s) and the source, provide a link to the Creative Commons licence, and indicate if changes were made. The images or other third party material in this article are included in the article's Creative Commons licence, unless indicated otherwise in a credit line to the material. If material is not included in the article's Creative Commons licence and your intended use is not permitted by statutory regulation or exceeds the permitted use, you will need to obtain permission directly from the copyright holder. To view a copy of this licence, visit http://creativecommons.org/licenses/by/4.0/.

Graphical abstract



Background

Historically, many studies have shown that medicinal plants are an essential source for discovering new natural compounds with unique structures and pharmacological properties. Therefore, the interest in natural compounds as a source for drug discovery has been widely studied in the last few years [1]. Many of these natural products have played a major contribution in drug discovery processes and have been widely used due to their effectiveness and low side effects compared with synthetic drugs [2].

The vascular plant family Asteraceae (Composite) is one of the biggest widespread families and includes 1100 genera and 25,000 species of herbaceous or shrubs that are widely located in tropical and subtropical regions. The natural metabolites of its genera are considered unique sources of biologically active compounds. *Euryops arabicus* is well known in the Arabian Peninsula as a traditional herbal medicine. It is characterized by a small erect undershrub of a height of up to one m [3]. The majority of isolated compounds from the plant belong to flavonoids, terpenes, and furoermophilanes skeletons as either steroidal or nonsteroidal conformation, and this wide range of chemical compounds might play an increasingly prominent role in the field of medicine [4].

Pharmacological studies have proven that the organic extract of the aerial parts of *Euryops arabicus* possesses potential biological activities, including anti-inflammatory and antitumor activities. For instance, the isolated kaurane diterpene (18,19-dihydroxy-kaura-16-en-3-one) and methoxylated flavones (7-hydroxy-3′,4′, 6,8-tetrtamethoxyflavone and 5-hydroxy-3′,4′,7-trimethoxyflavone) from chloroform–methanol extract were evaluated against tumor activities through different cancer cell lines (WI-38, VERO, HepG2, and MCF-7) and possessed significant antiproliferative activities against cells with IC_{50} in range 10–125 mM. The methylated moiety in flavones induced stronger activity compared to the diterpenes [5]. In addition, polymethoxylated flavonoid compounds isolated from the plant exhibited in *vivo* and in *vitro* anti-inflammatory activity in a rat injected with carrageenan in the plantar area and peripheral blood mononuclear cells (PBMCs), respectively [5]. The isolated furanoeremophilanes 6-isovaleryloxy-euryopsin, 6-isopropionyl euryopsin, (adenostylone), 6-senecioyl-euryopsin-9-on, 6-β-(2′-methyl-2′,3′-epoxy-butyryloxy)-10-α-H-9-oxofuranoeremophilane, and euryopsonol-senecioate compounds showed significant vasodilatory activities. The presence of an oxirane ring in furanoeremophilanes enhanced their vasodilatory effects [6]. Therefore, *Euryops arabicus* is a wealthy natural anticancer and anti-inflammatory drug-lead source.

The antimicrobial properties of some medicinal plants growing in various localities, especially *Euryops arabicus*, against human pathogenic microorganisms, were not well detected, and there was a strong correlation between plant chemical composition, biological properties, and geographic plant distribution [7]. The essential oil derived from *E. arabicus* is rich in oxygenated sesquiterpenes and has demonstrated antimicrobial activity against various bacteria, with minimum inhibitory concentration (MIC) values ranging from 0.32 to 5.25 mg/mL [8]. This antimicrobial effect assists in preventing biofilm formation through at least two mechanisms: inhibiting cell division and interfering with quorum sensing. Biofilm formation typically occurs in four stages, beginning with the adhesion of primary colonizers (such as planktonic cells) to a surface and the subsequent production of a conditioning

film. Disrupting this initial stage, for instance by inhibiting microbial growth, maybe a key strategy in preventing the establishment of bacterial biofilms [9].

The bacterial biofilms are more challenging to treat than their planktonic cells due to the form of a complex of polysaccharides, proteins, and other organic components. Biofilms enable microbes that attach to a surface to persist even in severe conditions. Therefore, bacterial biofilm formation is one of the indirect mechanisms that enhances bacteria resistance to antibiotics and can transfer resistance genes within the bacterial members of the biofilm. The genera *Escherichia*, *Staphylococcus*, *Pseudomonas*, *Pasteurella*, *Bacillus*, and *Salmonella* cause infections that are difficult to treat due to their ability to form biofilms. Therefore, searching for potential drugs is a promising method that leads to many new approved natural antibacterial products and their derivatives [10–13].

Studies on the compounds and biological activities of *E. arabicus* remain limited. A search in Scopus, SciFinder, and Web of Science databases retrieved 21, 18, and 13 documents, respectively (accessed on February 25th, 2025). The isolation of compounds such as furanoeremophilanes and eremophilanolides has been conducted since the 1980s; however, these studies primarily focused on structure elucidation without biological testing [14]. Research on the antimicrobial properties of *E. arabicus* has mostly utilized crude extracts from methanol or mixed organic solvents without further compound isolation [4, 15, 16]. In contrast, the isolation and characterization of diterpenes and flavones from this species have been performed specifically for in vitro anticancer investigations [3]. Other studies have explored different biological activities, including antioxidant and anti-inflammatory activities [6, 17]. However, in silico studies are absent from most of the existing literature. Therefore, a comprehensive investigation of *E. arabicus* compounds with antimicrobial, biofilm-preventive, and anticancer properties, along with in silico analysis, is highly warranted. The major endeavor of the current work is to analyze the chemical composition of the Saudi plant *E. arabicus* and evaluate the antimicrobial and anticancer activities of its metabolites.

Materials and methods

General

Merck silica gel 60 columns and thin-layer chromatography (TLC) using Merck silica gel 60 F_{254} 0.25 mm thickness plates (Macherey–Nagel) were used. All commercial solvents and reagents were obtained from various commercial suppliers (Honeywell and Sigma) and used without further purification. The visualizing agent on TLC was UV light (254 nm) and 50% sulfuric acid in methanol as spraying reagent followed by heating at 150 °C for 1–2 min BRUKER Unity INOVA 600 MHz instrument used for detection of nuclear magnetic resonance spectra (^{1}H-NMR, ^{13}C NMR, and 2D) at 25 °C. Deuterated chloroform ($CDCl_3$, Sigma-Aldrich) was used as a solvent.

Plant material

The aerial parts of *Euryops arabicus* were collected on August 27, 2021, from Al-Swdah, Abha, located in the southern part of the Kingdom of Saudi Arabia (18° 10′ 16.5″ N; 42° 25′ 55.7″ E). A voucher specimen was deposited in the collection of the Chemistry Department, Faculty of Science, KAU, Jeddah, Saudi Arabia.

Extraction and isolation

The dried aerial parts of the plant (2501.4 g) were extracted twice with a mixture of *n*-hexane, methanol, and chloroform (1:1:1, 15 L; 3 times) at 22 °C for 3 days. The combined extracts were filtered and concentrated to dryness, yielding a dark green residue (168.75 g; coded FE).

The extract (40 g) was further fractionated through column chromatography on silica gel. Gradient elution was carried out with gradation of polarities starting from *n*-hexane to *n*-hexane: diethyl ether mixtures to yield 60 fractions (1.FE–60.FE), followed by mixtures of *n*-hexane: ethyl acetate to yield 181 fractions (61.FE–242.FE), then by dichloromethane: methanol to yield 97 fractions (243.FE–340.FE). The fraction eluted with pure *n*-hexane afforded compound **3** (R_f 0.85) after purification with PTLC (5% diethyl ether in *n*-hexane). The fraction eluted with *n*-hexane: diethyl ether (95:5, v/v) afforded compound **2** (R_f 0.70) after purification with PTLC (10% diethyl ether in *n*-hexane). The fraction eluted with *n*-hexane: ethylacetate (85:15, v/v) afforded compounds **1** (R_f 0.63) and **4** (R_f 0.52) after purification with PTLC (20% ethylacetate in *n*-hexane).

Molecular docking experiment

Molecular docking experiments were conducted to assess both antibacterial and anticancer activities. For the antibacterial experiment, the proteins selected included D-amino acid aminotransferase (D-AAAT), methionyl-tRNA synthetase (MetRS), DNA gyrase, and penicillin-binding protein 1a (PBP1a). Meanwhile, the anticancer experiment focused on epidermal growth factor receptor (EGFR), vascular endothelial growth factor receptor 2 (VEGFR2), and B cell CLL/lymphoma 2 (Bcl-2). The 3D structures of these proteins were obtained from the RCSB Protein Data Bank (PDB) (https://www.rcsb.org, accessed on 17 October 2023). As for compounds **1–4**, their 3D conformers were generated using ChemDraw®, followed by energy minimization using the same software. Prior to

the docking experiments, thorough protein preparation and optimization were conducted using AutoDock4 and AutoDock1.5.7. This preparation included removing cofactors, ions, and water molecules, adding polar hydrogen, and applying Kollman charges to ensure precise docking accuracy [18]. Similarly, compounds **1–4** were optimized using these tools. Subsequently, molecular docking experiments were executed using the aforementioned software. To validate the docking experiments, redocking of native ligands was performed.

Molecular dynamic simulation

The NAMD program, developed by the Theoretical and Computational Biophysics Group, the NIH Center for Macromolecular Modeling and Bioinformatics, and the Beckman Institute of the University of Illinois, Urbana-Champaign, Illinois, USA, was employed to execute molecular dynamics (MD) simulations [19]. The CHARMM-GUI web server (https://charmm-gui.org, accessed on 20 October 2023) was applied to prepare the proteins and ligands [20–22]. A TIP3P water box extending 12 Å from the edge of proteins was utilized for the explicit solvation of proteins and their complexes. A standard protocol involving energy minimization and system equilibration was executed before initiating MD simulations using NAMD. The equilibration of water continued until convergence was achieved for both temperature and total energy. Periodic boundary conditions (PBCs) were maintained throughout each system's 100 ns (ns) MD simulations. The simulations were carried out with a time step of 2 femtoseconds (fs). A van der Waals and electrostatics cutoff of 14 Å was set, with a switching function within 2 Å. To maintain the system at a temperature of 310 K and a pressure of 1 atm, the isothermal-isobaric (NPT) ensemble was utilized. Temperature control was implemented using a Langevin thermostat, while pressure regulation employed the Nose–Hoover Langevin piston method [23]. Visualization of molecular dynamics was performed using the visual molecular dynamics (VMD) program developed by the Theoretical and Computational Biophysics Group, the NIH Center for Macromolecular Modeling and Bioinformatics, Beckman Institute, University of Illinois at Urbana-Champaign, Illinois, USA [24].

Antibacterial assay

The antimicrobial activities of the isolated compounds were tested against some Gram-positive and Gram-negative bacteria obtained from King Fahd General Hospital, Jeddah, Saudi Arabia, using the agar well diffusion method of Holder and Boyce [25].

Biofilm assay

All collected bacterial isolates were screened and assayed for biofilm formation using the crystal violet staining (CVS) method described by Christensen et al. (1995), and the ability to form biofilm was measured [26]. Broth cultures were incubated in 96-well microplates under standard conditions. The biofilm biomass was assayed as described before, and the percentage of inhibition was estimated [27].

Cell culture

Adenocarcinoma (MCF-7), hepatocellular carcinoma (HepG2), and colon cancer (HCT116) cell lines were obtained from the American Type Culture Collection (ATCC) (Manassas, VA, USA). The cell lines were cultured in the Eagle's Minimum Essential Medium (MCF-7 and HepG2) or McCoy's 5A (HCT116) that contained penicillin (100 U/mL), streptomycin (100 µg/mL), and heat-inactivated fetal bovine serum (FBS; 10%). The cells were propagated in a humidified cell culture incubator with 5% (v/v) CO_2 at 37 °C.

Cell viability assay

Cell viability was assayed by the sulforhodamine B (SRB) as previously reported [28].

Cell cycle analysis

The effect of the isolated compounds and the total extract on the cell cycle distribution of MCF-7, HepG2, and HCT 116 cells was determined by using flow cytometry analysis (FCA). Except for the control group, cells were subjected to the pre-determined IC_{50} isolates for 48 h. After incubation, the cells were collected by trypsinization, washed twice with ice-cold PBS, and resuspended in 0.5 ml of PBS. 60% ice-cold ethanol (2 ml) was added gently while vortexing, and cells were incubated for fixation at 4 °C for 1 h. Upon analysis, the fixed cells were washed and resuspended in 1 ml of PBS containing 50 µg/ml RNase A and 10 µg/ml propidium iodide (PI), after 20 min of incubation in darkness at 37 °C. Finally, FACS analysis was performed using a Cytek® Northern Lights 2000 spectral flow cytometer (Cytek Biosciences) using SpectroFlo™ Software version 2.2.0.3 (Cytek Biosciences), USA, was used to evaluate the data from 10,000 cells and the distribution of cell cycle phases for each sample.

Annexin V staining

The effects of compounds 1–4, in addition to the total extract, on apoptosis and necrosis of the studied cell lines were determined by flow cytometry analysis using a Cytek® Northern Lights 2000 spectral flow cytometer

(Cytek Biosciences) and SpectroFlo™ Software version 2.2.0.3 (Cytek Biosciences), USA. The method was conducted as previously reported [29].

Statistical analysis

Data were analyzed using one-way analysis of variance (ANOVA) followed by Tukey test. Differences between groups were considered significant at $p < 0.05$. Graphs were plotted using GraphPad Prism software, version 8.00 (GraphPad Software, La Jolla, CA, USA).

Results

Phytochemical characterization

Chromatographic purification of the organic extract obtained from the semi-dried whole plant of *E. arabicus* yielded four furano-based sesquiterpenoids, sesquiterpenoids identified as 6β-senecioyloxy-1,10-dehydrofuranoeremophilan-9-one (**1**), 6β-acetoxy-9-oxoeuryopsin (**2**), 6β-(2′-methyl, 2′,3′-epoxy-butyryloxy)-euryopsin (**3**), and 6β-angloyloxy-1,10-dehydrofuranoeremophilan-9-one (**4**) (Fig. 1).

6β-senecioyloxy-1,10-dehydrofuranoeremophilan-9-one (1)

Colorless oil (11 mg); ^{1}H-NMR (600 MHz, $CDCl_3$): δ 7.0 [1H, t, *J* = 3.6 Hz H-1], 2.25 [1H, m, Ha -2], 2.25 [1H,m, Hb-2], 1.55 [1H, m, Ha-3], 1.56 [1H, m, Hb-3], 1.98 [1H, m, H-4], 6.40 [1H, *s*, H-6], 7.40 [1H, *s*, H-12], 1.88 [3H, s, H-13] 1.13 [3H, *s*, H-14], 0.98 [3H, *d*, *J* = 6.8 Hz, H-15], 5.80 [1H, s, H-2'], 2.25 [3H, s, H-4'], 1.98 [3H, s, H-5']; ^{13}C NMR (125 MHz, $CDCl_3$): δ 176.51 (C-9), 145.9 (C-8), 146 (C-12), 137.99 (C-7), 121.17 (C-11), 74.9 (C-6), 135.79 (C-1), 141.38 (C-10), 46.6 (C-5), 37.17 (C-4), 24.72 (C-2), 27.8 (C-3), 15.88 (C-14), 17.49 (C-15), 8.8 (C-13), 166.16 (C-1'), 127.20 (C-2'), 159.74 (C-3'), 18.72 (C-4'), 20.57 (C-5').

6β-acetoxy-9-oxoeuryopsin (2)

Colorless oil (23 mg); ^{1}H-NMR (600 MHz, $CDCl_3$): δ 6.87 [1H, brs, H-1], 2.25–2.28 [2H, m, H-2], 1.74 [1H,m, Ha-3], 1.76 [1H, m, Hb-3], 1.98 [1H, m, H-4], 6.43 [1H, *s*, H-6], 7.40 [1H, *s*, H-12], 1.91 [3H, s, H-13] 1.00 [3H, *s*, H-14], 1.17 [3H, *d*, *J* = 6.8 Hz, H-15], 2.05 [3H, s, CH_3CO]; ^{13}C NMR (125 MHz, $CDCl_3$): δ 176.6 (C-9), 176.4 (**C**OCH_3), 146.4 (C-8), 146.5 (C-12),141 (C-10), 139.0 (C-1), 135.9 (C-7), 121.3 (C-11), 73.2 (C-6), 47.1 (C-5), 34.3 (C-3), 27.2 (C-4), 24.7 (C-2), 19 (**C**H_3CO), 18.6 (C-15), 15.1 (C-14), 8.7 (C-13).

6β-(2′-methyl, 2′,3′-epoxy-butyryloxy)-euryopsin (3)

Colorless oil (4 mg) $C_{20}H_{24}O_5$ HRESIMS *m/z* 345.1695 (calculated for $C_{20}H_{24}O_5$ $[m+1]^+$, 345.1688), ^{1} H-NMR: *δ* 6.96 (1H, m, H-1), 1.49 (1H, m, H-2), 1.65 (1H, m, H-2), 2.22 (1H,m, H-3), 2.29 (1H, m, H-3), 1.93 (1H, m, H-4), 6.48 (1H,s,H-6), 7.41 (1H, s, H-12), 1.95 (3H, s, H-13), 1.16 (3H, s, H-14), 0.99 (3H, d, *J* = 6.8 Hz, H-15), 3.16 (1H, m, H-3'), 1.48 (3H, d, *J* = 6.8 Hz, H-4'), 1.66 (3H, s, H-5'). ^{13} C NMR: *δ* 177.1 (C-9), 169.8 (C-1'), 147.1 (C-8), 145.9 (C-12), 141.0 (C-10), 138.1 (C-1), 134.9 (C-7), 134.9 (C-11), 75.41 (C-6), 61.3 (C-3'), 58.8 (C-2'), 47.0 (C-5), 36.0 (C-4), 27.6 (C-2), 24.0 (C-3), 19.5 (C-5'), 16.3 (C-14), 13.4 (C-4'), 8.8 (C-13).

6β-angloyloxy-1,10-dehydrofuranoeremophilan-9-one (4)

Colorless oil (18 mg); HREIMS: *m/z* 328.1686 $[M]^+$; calcd. For $C_{20}H_{24}O_4$, ^{1}H-NMR (600 MHz, $CDCl_3$): δ 7.0 [1H, t, *J* = 3.6 Hz H-1], 2.33 [1H, m, Ha -2], 2.33 [1H,m, Hb-2], 1.55 [1H, m, Ha-3], 1.56 [1H, m, Hb-3], 1.99 [1H, m, H-4], 6.43 [1H, *s*, H-6], 7.39 [1H, *s*, H-12], 1.87 [3H, s, H-13] 1.13 [3H, *s*, H-14], 0.98 [3H, *d*, *J* = 6.8 Hz, H-15], 6.28 [1H, qq, *J* = 6.0, 1.4 Hz, H-3'], 2.10 [3H, dq, *J* = 5.8, 1.5 Hz, H-4'], 1.99 [3H, s, H-5']; ^{13}C NMR (125 MHz, $CDCl_3$): δ 176.6 (C-9), 145.9 (C-8), 146.82 (C-12), 136.04

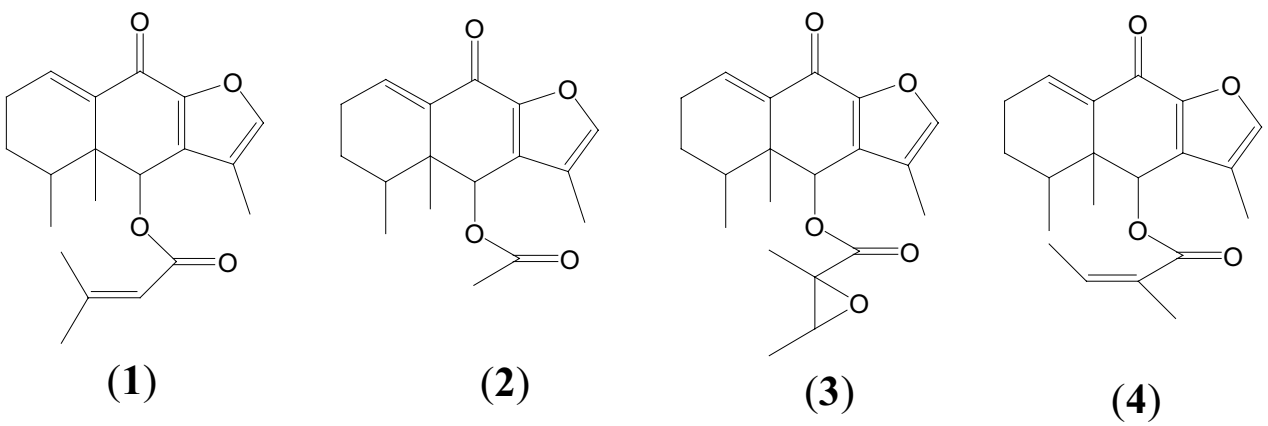


Fig. 1 Compounds isolated from *E. arabicus*

(C-7), 121.19 (C-11), 73.9 (C-6), 138.27 (C-1), 141.36 (C-10), 46.6 (C-5), 37.8 (C-4), 25.17 (C-2), 27.9 (C-3), 15.55 (C-14), 17.50 (C-15), 8.4 (C-13), 167.07 (C-1'), 126.98 (C-2'), 141.65 (C-3'), 16.06 (C-4'), 20.57 (C-5').

Molecular studies

The data in Table S1 represented the selected protein and the respective root-mean-square deviation (RMSD) from the re-docking of native ligands. The RMSD value < 2 Å in all re-docking of native ligands indicated the docking procedure used in this study was valid.

The binding energy of compounds **1–4** exhibited negative values for all the targeted anticancer and antibacterial properties, indicating their potential to bind to the respective proteins. In the anticancer docking experiment, the binding energies of compounds **1–4** to 1M17 were the most substantial, ranging from − 7.2 to − 7.8 kcal/mol. Doxorubicin binding, used as a standard drug, to 1M17, displayed the highest binding energy at -10.6 kcal/mol (Table S2).

Interestingly, all bounds of compounds **1–4** to 1M17 were established by hydrophobic interaction only. The visualization of compound **1** with 1M17 docking interactions indicated 9 hydrophobic interactions as one Pi-sigma, five alkyl, and three Pi-alkyl types. The docking of compound **2** with 1M17 revealed the presence of 8 hydrophobic interactions. Thirteen hydrophobic interactions were observed in the docking of compound **3** with 1M17, ranging in distance from 3.55 to 5.44 Å. Similarly, 13 hydrophobic interactions were observed in docking compound **4** with 1M17 (Table S3; Fig. S1).

Meanwhile, compounds **3** and **4** demonstrated their highest binding affinities with protein 1P7P, with binding energies of − 7.7 and − 7.8 kcal/mol, respectively. It is noteworthy that amoxicillin, a widely used antibacterial agent, also exhibited a strong binding affinity with 1P7P, with a binding energy of -8.6 kcal/mol (Fig. S3).

Compound **1** to 1P7P docking was established by two hydrogen bonds, one electrostatic interaction, and five hydrophobic interactions. In compound **2** with 1P7P docking, four hydrogen bonds, six hydrophobic bonds, and two electrostatic bonds are present. The hydrogen bonds were established between oxygen atoms and ASP296 (2.65 Å), ILE297 (2.71 Å), GLY23 (3.47 Å), and HIS24 (3.50 Å). The interactions of compound **3** with 1P7P consisted of four hydrogen bonds, with distances ranging from 2.00 to 2.71 Å. In addition, six hydrophobic interactions were identified, spanning distances from 3.66 to 5.24 Å. The docking of compound **4** with 1P7P was supported by four hydrogen bonds involving various atoms from compound **4**, i.e., VAL326, GLY23, and TYR325. Additionally, seven hydrophobic interactions with MET333, LYS332, VAL326, HIS21, and TYR325 were noted, with distances within the range of 1.93–5.37 Å (Fig. S4).

Molecular dynamic simulations were conducted for compounds exhibiting the highest affinity to their respective proteins. The results of molecular dynamic simulations regarding root-mean-square deviation (RMSD) and root-mean-square fluctuation (RSMF) were presented. Molecular dynamic simulations with the anticancer target protein 1M17, the RMSD values were as follows: 1.40 ± 0.16 Å; 1.22 ± 0.11 Å, 1.37 ± 0.17 Å, and 1.41 ± 0.18 Å for compounds **1–4**, respectively. The fluctuation in the RMSD values displayed no significant alterations. It remained below 2 Å throughout 100 ns, indicating the stable complexation of compounds **1–4** with the protein target throughout the simulation (Fig. S3a). In the RSMF analysis of compounds **1–4** with 1M17, a similar fluctuation trend was observed in the sequence residues that interacted with the compounds. The residues 304–309 exhibited the highest fluctuation, particularly in the loop region (Fig. S3c). Molecular dynamic simulations involving the antimicrobial target protein 1P7P, the RMSD values were recorded as 1.21 ± 0.24 Å, 1.09 ± 0.12 Å, 1.05 ± 0.17 Å, and 1.04 ± 0.09 Å for compounds **1–4**, respectively. These RMSD values also demonstrated fluctuations below 2 Å, indicating that all three compounds maintained stable complexation with 1P7P throughout the simulation period (Fig. S3b). The RSMF analysis of compounds 1–4 with 1P7P observed a similar fluctuation pattern in the sequence residues. The highest fluctuation was observed in the loop region, specifically involving residue 155–160 (Fig. S3d).

Antimicrobial activity

Antimicrobial activity (diameter of inhibition zone, mm) of the tested fractions was determined and compared to amoxicillin (+ve control) on some multidrug-resistant bacteria using the agar well diffusion method (Table 1). Compounds **2** and **4** were more effective against all the tested bacteria compared to 3, which showed the lowest activity (inhibition zone diameters ranged from 9.0 to 10.0 mm while it ranged from 12.1 to 16.2 mm for 2 and from 12.9 to 19.0 mm for 4.

The two compounds, **2** and **4**, showed great inhibitory activity for the two bacterial species, *Pseudomonas aeruginosa and Staphylococcus aureus*. These two species are well known to form strong biofilm on different surfaces, making them difficult to treat. The recorded MICs ranged from 12.5 to 25.0 µg/ml. Low MIC was recorded for compound **4,** which indicates a high antimicrobial activity (Table 2). Compounds **2** and **4**, at a concentration of 1/2 MIC, inhibited biofilm formation by *P. aeruginosa* by 55 and 50%, respectively, while the recorded inhibition percentages were 58 and 79% for *S. aureus.*

Table 1 Antimicrobial activity (diameter of inhibition zone, mm) of the tested fractions compared to amoxicillin (control antibiotic) on some multidrug-resistant bacteria using agar well diffusion method

Bacterium	Compounds			Control
	2	3	4	
Gram-negative				
E. coli	19.0 ± 0.44	9.0 ± 0.4	14.1 ± 0.12	29.0 ± 0.49
K. pneumoniae	16.2 ± 0.42	9.0 ± 0.2	13.1 ± 0.23	29.5 ± 0.29
P. mirabilis	16.8 ± 1.01	9.0 ± 0.5	16.0 ± 0.33	27.3 ± 0.98
P. aeuroginosa	16.8 ± 1.30	9.1 ± 0.5	15.0 ± 1.49	27.3 ± 0.89
Gram positive				
E. faecalis	14.7 ± 0.39	9.1 ± 1.0	14.0 ± 0.53	44.9 ± 0.99
MRSA	12.9 ± 0.66	9 .3 ± 0.0	13.4 ± 0.11	20.9 ± 0.77
S. aureus	12.9 ± 0.20	10.3 ± 0.1	16.2 ± 0.23	45.3 ± 0.33
Streptococcus pyogenes	14.0 ± 0.49	10.0 ± 0.4	16.0 ± 0.40	46.0 ± 0.39

*Amoxicillin: positive control; mean ± SD (n = 3), MRSA: *Methicillin-resistant Staphylococcus aureus*

Table 2 The minimal inhibition concentration–MIC (µg/mL) and percentage of biofilm inhibition compared to negative control of the two compounds extracted from *E. arabicus*

Bacterium	2		4	
	MIC	% BFI_2	MIC	% BFI_4
P. aeruginosa	25.0	55	12.5	50
S. aureus	25.0	58	12.5	79

%BFI: Percentage of bacterial biofilm inhibition compared to negative control

Table 3 Cytotoxic effects of the isolated metabolites (**1–4**)

Compound No	IC_{50} (mean ± SD; n = 3; µg/L)		
	MCF-7	HepG2	HCT 116
1	6.94 ± 1.47	1.29 ± 0.22	2.00 ± 0.24
2	1.78 ± 0.49	1.42 ± 0.13	2.82 ± 0.13
3	2.15 ± 0.09	2.18 ± 0.16	15.8 ± 2.41
4	3.23 ± 0.16	1.48 ± 0.28	8.23 ± 0.71
Total extract	1.63 ± 0.28	0.78 ± 0.19	6.75 ± 0.92
Doxorubicin	1.03 ± 0.02	1.08 ± 0.01	1.5 ± 0.09

Antiproliferative activity

Table 3 displays the antiproliferative activities of compounds **1–4** as well as the total organic extract of *E. arabicus*. In general, compound **2** showed a high antiproliferative effect against all examined cell lines, while compound **1** showed potent activity against HepG2 and HCT 116 cells. Compounds **3** and **4** showed high activity against MCF-7 and HepG2 cells and marginal activities against HCT 116 cells.

Cell cycle analysis

DNA content analysis using flow cytometry was employed to investigate the impact of all isolates on cell cycle progression. In MCF-7 cells, both **2** and the total extract caused a significant cell cycle arrest at the G2 phase at 48 h after treatment. The percentage of cells in the G2 phase increased notably from 48.6 ± 0.5 to 64.1 ± 1.8% with the **2** and from 48.6 ± 0.5 to 61.4 ± 1.7% with the total extract. Furthermore, the **1** and **3** arrested cells in the S phase, increasing the percentage from 40.6 ± 1.5 to 54.8 ± 1.3% with the **1** and from 40.6 ± 1.5 to 59.4 ± 1.8% with the **3**. In HepG2 and HCT116 cells, **1** significantly increased the G2 phase cell population after 48 h of treatment. The percentage of cells in the G2 phase rose from 1 ± 0.02 to 68.4 ± 1.6% in HepG2 cells and from 47.9 ± 1.7 to 75.3 ± 1.9% in HCT116 cells. Additionally, **2** influenced HCT116 cells, causing an increase in cell arrest at the G2 phase. Similarly, **4** also induced G2 arrest in HepG2 cells, increasing the percentage of cells in the G2 phase up to 86.7 ± 2.3%. Interestingly, the total extract exhibited different effects on HepG2 and HCT116 cells. It caused cell cycle arrest at the S phase, increasing the percentage of cells in the S phase from 46.6 ± 1.4 to 87.9 ± 1.8% in HCT116 cells and from 49.5 ± 1.6 to 69.3 ± 1.3% in HepG2 cells. Similarly, **2** influenced S phase arrest after 48 h. In addition, **3** arrested cells at the G2 phase in HepG2 cells, increasing the percentage up to 58.3 ± 1.8%, while it affected cell arrest at the G1 phase in HCT116 cells, increasing the percentage from 5.4 ± 0.09 to 70.9 ± 1.8% (Fig. 2).

Annexin V staining

Annexin V/FITC-PI staining combined with flow cytometry was used to evaluate apoptosis and necrosis in the treated cells. Our data revealed that all compounds and the total extract had a significant capacity to induce apoptosis in all three cancer cell lines (MCF-7, HePG2, and HCT116) after 48 h of exposure. Specifically, **2** and **4** exhibited a strong pro-apoptotic effect on MCF-7 cells compared to other compounds, with a total apoptotic percentage of approximately 94.87 ± 1.9%. Moreover, **3** and the total extract demonstrated potent apoptotic effects on MCF-7 cells compared to the control. In contrast, a notably high necrotic effect was observed in MCF-7 cells, accounting for 27.27 ± 0.9% compared to the necrotic percentage after treatment with other cancer cells. In HepG2 cells, **2**, **3**, and the total extract significantly enhanced cell death activity, with an apoptotic percentage of around 94.6 ± 1.9% compared to the **1** and **4**. Additionally, **4** induced necrotic activity,

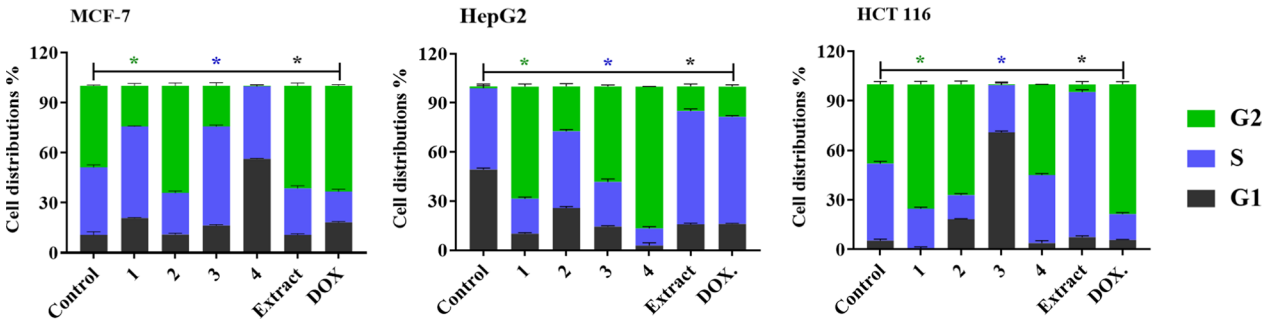


Fig. 2 Cell cycle phases (mean ± SD; $n = 3$) of MCF-7, HepG2, and HCT 116 after compounds **1–4** and total extract exposure. After 48 h of exposure, DNA cytometry analysis was used to identify the cell cycle distribution. *$p < 0.05$

resulting in 7.2 ± 0.3% necrotic cells compared to other extracts. Although a lower percentage of apoptotic cells were observed in HCT116 cells after treatment with isolates compared to other cancer cells, they exhibited apoptotic effects compared to the control. **1**, **2**, and **3** compounds showed an apoptotic percentage of approximately 84.5 ± 1.7%, while necrosis was observed in the **1** and the total extract samples compared to other compounds (Fig. 3).

Discussion

This study discussed the isolation of four furano-sesquiterpenes from *E. arabicus.* Compound **1** was isolated as colorless oil. The molecular formula was indicated by HREIMS: *m/z* 328.1686 $[M]^+$, calculated for $C_{20}H_{24}O_4$. The ^{13}C-NMR spectrum accounted for 20 carbons. With the aid of DEPT experiment the carbon atom signals were categorized into eight quaternary carbons resonating at δ 176.5, 166.1, 159.7, 145.9, 141.3, 137.9, 121.1, and 46.6 ppm, five methine carbon signals at 146, 135.7, 127.2, 74.3, and 37.1 ppm two methylene carbon signals appeared at 27.8 and 24.7 ppm, and five methyl signals. HSQC spectrum indicated the J^1 attachments. The compound contains two carbonyl carbons and four carbon–carbon double bonds. The presence of a de-shielded methine signal at δ_H/ δ_C 7.40/146 and δ_C 145.9 ppm suggested the presence of a trisubstituted furan group. In addition, NMR data showed the presence of an senecioyl group [δ_H 5.80 (1H, s, H-2'), 2.25 (3H, s, H-4'), 1.98 (3H, s, H-5'), δ_C 167.07 (C-1'), 166.16 (C-1'), 127.20 (C-2'), 159.74 (C-3'), 18.72 (C-4'), 20.57 (C-5'). ^{1}H-^{1}H COSY spectrum assigned the presence of a single sequence CH(1)-CH_2(2)-CH_2(3)-CH(4)-CH_3. The presence of furoeremorphilan carbon skeleton is expected when studying the constituents of *E. arabicus*. The in-hand spectral data showed compound **1** was identical to 6β- senecioyloxy-1,10-dehydrofuranoeremophilan-9-one [30].

Compound **2** was isolated as optically active oily material. The structure elucidation of compound **2** commenced with measuring the ^{1}H-NMR spectral data, three proton signals were observed in the downfield region of the spectra resonating at δ 7.40, 7.01, and 6.42 ppm, three tertiary methyl functions resonating at 2.05, 1.91, and 1.0 ppm, a secondary methyl group observed at 1.17 ppm (d, 6.8 Hz), and five signals at 2.28, 2.24, 1.66, 1.47 and 2.03 ppm. The molecular formula of compound **2** was established as $C_{17}H_{20}O_4$, implying eight degrees of unsaturation. ^{13}C-NMR spectrum displayed fifteen carbon atom signals that were classified by DEPT experiment into seven quaternaries (δ 176.6, 176.4, 146.4,

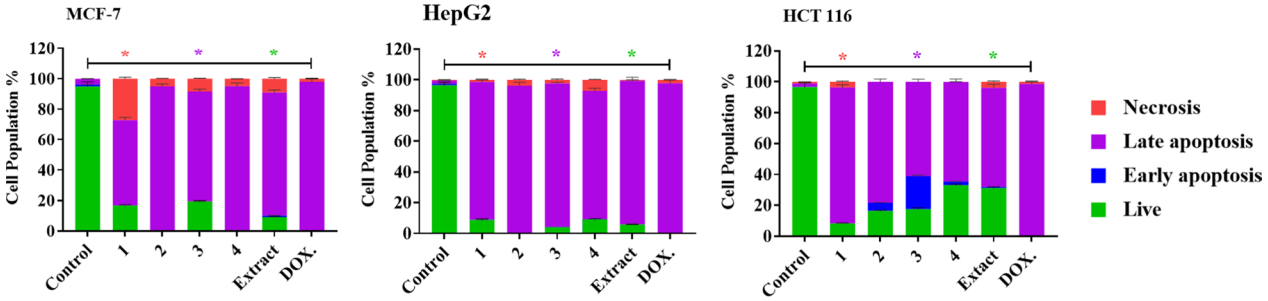


Fig. 3 The apoptotic effect of compounds **1–4** and total extract (mean ± SD; $n = 3$) on the cell apoptosis in MCF-7, HepG2, and HCT 116 cancerous cells by Annexin V-FITC/PI labeling by flow cytometry. Exposure to treatments for 48 h. **$p < 0.01$ and ***$p < 0.001$

141, 135.9, 121.3, and 47.8 ppm), four methines (145.9, 138.5, 74.4, and 27.2 ppm), two methylene (34.3 and 24.7 ppm), and four methyl carbon signals (19, 15.1, 18.6, and 8.7 ppm). HSQC spectrum indicated the J^1 attachments. The compound contains two carbonyl carbons and three carbon–carbon double bonds, which leave three sites unsaturated for the tricyclic structure. The presence of a de-shielded methine signal at δH/ δC 7.40/146.5 and δ_C 146.4 ppm suggested the presence of a trisubstituted furan group. The absence of any other oxygenated function group assigned a tricyclic structure, including a fused trisubstituted furan ring. ^{1}H-^{1}H COSY spectrum assigned the presence of a single sequence CH(1)-CH_2(2)-CH_2(3)-CH(4)-CH_3. The presence of furoeremorphilan carbon skeleton is expected when studying the constituents of *E. arabicus*. The in-hand spectral data are in agreement with the previous published data for 6β-acetoxy-9-oxoeuryopsin (**2**) which were isolated from the same plant species [30].

Compound **3** was isolated as optically active oily material. The structure elucidation of compound **3** commenced with measuring the ^{1}H-NMR spectral data; two proton signals were observed in the downfield region of the spectra resonating at δ 7.41 and 6.96 ppm, two tertiary methyl functions resonating at 1.16 and 1.95 ppm, three secondary methyl group were observed at 0.99 (d, 6.8 Hz) 1.48 (d, 6.8 Hz), and at 1.66 (d, 6.8 Hz), along with a methine proton signal at 3.16 (d, m). The molecular formula of compound **3** was established as $C_{20}H_{24}O_5$, implying nine degrees of unsaturation. ^{13}C-NMR spectrum displayed ninteen carbon atom signals that were classified by DEPT into eight quaternaries (δ 177.1, 169.8, 147.1, 145.9, 141.0, and 134.9, 134.9, 58.8, and 47.0 ppm), five methine (145.7, 138.1, 75.4, 61.3, and 36.0 ppm), two methylenes (27.6 and 24.0 ppm), and five methyl carbon signals (19.4, 17.2, 16.3, 13.4 and 8.8 ppm). HSQC spectrum indicated the J^1 attachments. The presence of a de-shielded methine signal at δH/ δC 7.41/145.9 and δ_C 134.9 ppm suggested the presence of a trisubstituted furan group. The presence of the two carbon signals at 61.1 and 58.8 together with the ^{1}H-NMR absorption signal at 3.16 ppm, suggested the presence of an oxirane ring. The proposed molecular formula and the NMR data assigned a tetracyclic structure, including a fused trisubstituted furan ring. ^{1}H-^{1}H COSY spectrum assigned the presence of a single sequence CH(1)-CH(2)-CH_2(3)-CH(4)-CH_3, the other protons appeared without cross-correlations. The in-hand spectral data agree with the previously published data for 6β-(2′-methyl, 2′,3′-epoxybutyryloxy)-euryopsin (**3**), which were isolated from the same plant species [30].

Compound **4** was isolated as colorless oil. The molecular formula was established as $C_{20}H_{24}O_4$ (HREIMS: *m/z* 328.1686 $[M]^+$; calcd. For $C_{20}H_{24}O_4$). The ^{13}C-NMR spectrum accounted for 20 carbons. With the aid of DEPT experiment the carbon atom signals were categorized into eight quaternary carbons resonating at δ 176.6, 167, 145.9, 141.36, 136.04, 126.98, 121.19, and 46.6 ppm, five methine carbon signals at 146.82, 141.65, 138, 73.9, and 37.8 ppm two methylene carbon signals appeared at 27.9 and 25.17 ppm, and five methyl signals. HSQC spectrum indicated the J^1 attachments. The compound contains two carbonyl carbons and four carbon–carbon double bonds, which leave four sites unsaturated for the tricyclic structure. The presence of a de-shielded methine signal at δ_H/ δ_C 7.39/146 and δ_C 145.9 ppm suggested the presence of a trisubstituted furan group. In addition, NMR data showed the presence of an angeloyl group [δ_H 6.28 (1H, qq, H-3'], 2.10 (3H, dq, H-4'), 1.99 (3H, s, H-5'), δ_C 167.07 (C-1'), 126.98 (C-2'), 141.65 (C-3'), 16.06 (C-4'), 20.57 (C-5'). The absence of any other oxygenated function group assigned a tricyclic structure, including fused trisubstituted furan ring. ^{1}H-^{1}H COSY spectrum assigned the presence of a single sequence CH(1)-CH_2(2)-CH_2(3)-CH(4)-CH_3. The presence of furoeremorphilan carbon skeleton is expected when studying the constituents of *E. arabicus*. The in-hand spectral data showed compound **4** was identical to 6β-angloyloxy-1,10-dehydrofuranoeremophilan-9-one. Compound **4** was previously reported from the Asteraceae plant *Senecio otites* [31].

Compounds **1–4** exhibited nearly identical cytotoxic properties, with compound **2** demonstrating the strongest cytotoxic effects across all tested cancer cell lines. Compound **3** displayed relatively weak cytotoxicity against HCT 116. Compounds **2** and **4** showcased the most potent antibacterial properties. Despite having identical core skeletons, these four compounds differ in their C-6 substitution patterns. Compound **2** contains an acetoxy group at C-6, which enhances its cytotoxicity. Compounds **1** and **4** share nearly identical substitution patterns, except for the methylation position—compound **1** has a methyl group at C-3', while in compound **4**, it appears at C-2'. Meanwhile, compound **3**, which features an oxirane ring, exhibits lower cytotoxicity and weaker antibacterial properties. Consequently, substitutions at C-6 in these isolated compounds significantly influence their biological properties. Another study found that the substitution pattern at C-1, C-6, and C-8 of eremophilanolides from various *Senecio* species impacts their cytotoxicity against human cancer cell lines [32]. The observed cytotoxic effects of compounds **1–4,** as well as the extract, were further substantiated by assessing their impact on cell cycle distribution. Our data indicated that the extract and compound **2** significantly enhanced cell fraction in the G2/m phase. This is

consistent with previous studies that highlighted the ability of sesquiterpenes as tomentosin, isoalantolactone, and atractylenolide-I to cause cell cycle arrest at G2/M phase [33]. However, compound **3** significantly enhanced the cell population in G1, which is in harmony with the ability of the sesquiterpene artemisinin to accumulate endometrial cancer cells in the G1 phase [34]. In addition, compounds **1** and **3** enhanced cell fraction in the S phase, an observation that gains support from the capability of acylfulvenes, a sesquiterpene derivative that induces DNA double-strand breaks and cell arrest in the S phase [35]. Furthermore, our data indicated that the observed cell phases were associated with pro-apoptotic activity, as evidenced by annexin V staining. In particular, late apoptosis was significantly enhanced by almost all test compounds and the total organic extract. This is supported by several studies demonstrating the pro-apoptotic activities of sesquiterpenes in cancer cells. These include gaillardin [36], isoalantolactone [37], and costunolide [38].

This study extensively evaluates the anticancer activities of isolated compounds **1–4** against MCF-7, HepG2, and HCT 116 cell lines; however, some limitations remain. While the study includes a detailed cell cycle analysis, it does not investigate other mechanisms of action, such as signaling pathways. Additionally, the antimicrobial and biofilm prevention activities were assessed, yet their underlying mechanisms were not thoroughly explored. Therefore, further studies are encouraged to investigate the mechanisms of anticancer activity in greater depth, particularly through signaling pathway analysis. Given the potent in vitro anticancer activity observed, in vivo studies are also recommended. Moreover, a more comprehensive examination of the antimicrobial and biofilm prevention properties is warranted. Biofilm formation involves at least four key stages: bacterial adhesion and surface conditioning, polymeric matrix production, biofilm maturation, and the release of persister cells from the biofilm [9]. Future research should explore how the isolated compounds influence each stage of biofilm formation to understand their potential applications in biofilm prevention better.

Conclusion

Eryopus arabicus, an endemic plant species in the Arabian Peninsula, has been shown to have the ability to produce phytochemicals with multiple pharmacological activities. Four furano-based sesquiterpenoids were isolated and characterized in the current study. Molecular docking studies indicated probable antibacterial and antiproliferative activities of the whole organic extract as well as the isolated metabolites. Experimentally, they displayed potent broad spectrum activities against Gram-negative and Gram-positive pathogens. In addition, these sesquiterpenoids showed powerful biofilm prevention for both *P. aeruginosa* and *S. aureus.* In addition, they exhibited potent antiproliferative effects against MCF-7, HepG2, and HCT116 human cancer cells. Collectively compound **2** showed a relatively high cytotoxic activity. This was associated with accumulation of the cancer cells in G2/M phase and enhancement of apoptotic cell death. Additional studies are recommended to further substantiate the observed activities.

Abbreviations

NMR	Nuclear magnetic resonance
UV	Ultraviolet
IR	Infrared
tRNA	Transfer ribonucleic acid
TLC	Thin-layer chromatography
PTLC	Preparative thin-layer chromatography
FE	Filtered extract
Rf	Retention factor
D-AAAT	D-amino acid aminotransferase
DNA	Deoxyribonucleic acid
PBP1a	Penicillin-binding protein 1a
EGFR	Epidermal growth factor receptor
VEGFR2	Vascular endothelial growth factor receptor 2
Bcl-2	B Cell CLL/lymphoma 2
RCSB	Research Collaboratory for Structural Bioinformatics
PDB	Protein Data Bank
MD	Molecular dynamic
NAMD	Nanoscale molecular dynamic
ns	Nanosecond
VMD	Visual molecular dynamics
CVS	Crystal violet staining
MCF-7	Michigan Cancer Foundation-7 (breast cancer cell lines)
HepG2	Hepatoblastoma cell lines
HCT116	Human colorectal carcinoma cell lines
FBS	Fetal bovine serum
CO2	Carbon dioxide
SRB	Sulforhodamine B
IC_{50}	Half-maximal inhibitory concentration
CDCl3	Deuterated chloroform
Hz	Hertz
δ	Chemical shift
brs	Broad singlet
m	Multiplet
d	Doublet
s	Singlet
J	Coupling constant
RMSD	Root-mean-square deviation
Å	Angstrom
RMSF	Root-mean-square fluctuation
MIC	Minimum inhibitory concentration
ppm	Part per million
DEPT	Distortionless enhancement by polarization transfer
HSQC	Heteronuclear single quantum coherence
COSY	Correlated spectroscopy

Supplementary Information

The online version contains supplementary material available at https://doi.org/10.1186/s43094-025-00810-w.

Additional file 1 (DOCX 534 KB).

Acknowledgements
The authors would like to thank the deanship of higher studies, King Abdulaziz University, for their support and help.

Author contributions
F.A.A, F.B.A, A.B.A, and F.B contributed to formal analysis; A.B.A, M.M.A, and W.M.A contributed to validation; F.A.A, N.O.B, H.I.A, and F.B contributed to writing-original draft; F.A.A and M.Y.A contributed to investigation; A.B.A, M.Y.A, M.M.A, and W.M.A contributed to conceptualization; A.B.A, M.M.A, and W.M.A contributed to methodology; W.M.A supervised the study; A.B.A and W.M.A contributed to writing-review and editing. All authors have read and approved the final manuscript. All authors contributed equally as the main authors for this manuscript.

Funding
This research received no specific grant from any funding agency in the public, commercial, or not-for-profit sectors.

Availability of data and materials
Required data and figures are available in the Supplementary Materials.

Declarations

Ethical approval and consent to participate
All authors approved this manuscript. The study does not include animals or human subjects.

Competing interest
The author declares that there is no conflict of interest.

Author details
[1]Department of Chemistry, Faculty of Science, King Abdulaziz University, PO. Box 80203, 21589 Jeddah, Saudi Arabia. [2]Department of Biological Sciences, Faculty of Science, King Abdulaziz University, PO. Box 80203, 21589 Jeddah, Saudi Arabia. [3]Department of Chemistry, Faculty of Science, Bisha University, PO Box 62562, Abha, Saudi Arabia. [4]Department of Chemistry, College of Science, University of Jeddah, 21589 Jeddah, Saudi Arabia. [5]Department of Pharmacology and Toxicology, Faculty of Pharmacy, King Abdulaziz University, 21589 Jeddah, Saudi Arabia. [6]Department of Biology, Faculty of Science, King Khalid University, 9004 Abha, Saudi Arabia. [7]Botany Department, Faculty of Science, Kafrelsheikh University, Kafr El Sheikh 33516, Egypt. [8]Research Center for Vaccine and Drugs, National Research and Innovation Agency (BRIN), Bogor 16911, Indonesia. [9]Department of Marine Chemistry, Faculty of Marine Sciences, King Abdulaziz University, PO. Box 80207, 21589 Jeddah, Saudi Arabia.

Received: 10 December 2024 Accepted: 21 April 2025
Published online: 19 May 2025

References

1. Alshamrani RI, Aly MM (2022) Screening of some local traditional plants for their antitumor and antibacterial activities against the global emergence of multi-drug resistant bacteria. Biosci Biotechnol Res Commun 15:279–287. https://doi.org/10.21786/bbrc/15.2.3
2. Newman DJ, Cragg GM (2020) Natural products as sources of new drugs over the nearly four decades from 01/1981 to 09/2019. J Nat Prod 83(3):770–803. https://doi.org/10.1021/acs.jnatprod.9b01285
3. Alarif WM, Abdel-Lateff A, Al-Abd AM, Basaif SA, Badria FA, Shams M, Ayyad SEN (2013) Selective cytotoxic effects on human breast carcinoma of new methoxylated flavonoids from *Euryops arabicus* grown in Saudi Arabia. Eur J Med Chem 66:204–210. https://doi.org/10.1016/j.ejmech.2013.05.025
4. Moustafa M, Siddiqui S, Alrumman S, Shati A, Al-Kahtani M (2018) Antimicrobial activity and heavy metals findings of *Euryops arabicus* (Jabur) leaves against plant and human pathogens. Pak J Agric Sci 55(4):787–792. https://doi.org/10.21162/PAKJAS/18.6649
5. Abdel-Lateff A, Alarif WM, Algandaby MM, Alburae NA, Abdel-Naim AB (2020) *Euryops arabicus* displays anti-inflammatory activities in experimental models. J Ethnopharmacol 247:112278. https://doi.org/10.1016/j.jep.2019.112278
6. Abdallah HM, El-Halawany AM, El-Bassossy HM (2019) Furanoeremophilanes from *Euryops arabicus* alleviate metabolic syndrome-associated exaggerated vasoconstriction via direct vasodilatation. Phytochem Lett 32:15–22. https://doi.org/10.1016/j.phytol.2019.04.015
7. Yavari N, Mazaheri-Assadi M, Mazhari ZH, Moghadam MB, Larijani K (2018) Glucuronic acid rich kombucha-fermented pomegranate juice. J Food Res 7:61–69. https://doi.org/10.5539/jfr.v7n1p61
8. Mothana RA, Alsaid MS, Al-Musayeib NM (2011) Phytochemical analysis and In Vitro antimicrobial and free-radical-scavenging activities of the essential oils from *Euryops arabicus* and Laggera decurrens. Molecules 16:5149–5158. https://doi.org/10.3390/molecules16065149
9. Hussaini IM, Oyewole OA, Sulaiman MA, Dabban AI, Sulaiman AN, Tarek R (2024) Microbial anti-biofilms: types and mechanism of action. Res Microbiol 175:104111. https://doi.org/10.1016/j.resmic.2023.104111
10. De La Fuente-Núñez C, Cardoso MH, De Souza CE, Franco OL, Hancock REW (2016) Synthetic antibiofilm peptides. Biochim Biophys Acta Biomembr 1858:1061–1069. https://doi.org/10.1016/j.bbamem.2015.12.015
11. Betts JW, Hornsey M, La Ragione RM (2018) Novel antibacterials: alternatives to traditional antibiotics. Adv Microb Physiol 73:123–169. https://doi.org/10.1016/bs.ampbs.2018.06.001
12. Brown DG, Lister T, May-Dracka TL (2014) New natural products as new leads for antibacterial drug discovery. Bioorg Med Chem Lett 24:413–418. https://doi.org/10.1016/j.bmcl.2013.12.059
13. Romulo A, Zuhud EAM, Rondevaldova J, Kokoska L (2018) Screening of in vitro antimicrobial activity of plants used in traditional indonesian medicine. Pharm Biol 56:287–293. https://doi.org/10.1080/13880209.2018.1462834
14. Hafez S, Jakupovic J, Bohlmann F, Sarg TM, Omar AA (1989) Transformation products of furoeremophilanes and other constituents from *Euryops arabicus*. Phytochemistry 28(3):843–847. https://doi.org/10.1016/0031-9422(89)80126-8
15. Gouda YG, Abdallah QMA, Elbadawy MF, Basha AA, Alorabi AK, Altowerqe AS, Mohamed KM (2014) Cytotoxic and antimicrobial activities of some compositae plants growing in Taif Area, Saudi Arabia. Int J Pharm Sci Invent 3(5):43–48
16. Mothana RAA, Lindequist U (2005) Antimicrobial activity of some medicinal plants of the island Soqotra. J Ethnopharmacol 96:177–181. https://doi.org/10.1016/j.jep.2004.09.006
17. Abdel-Lateff A, Abdel-Naim AB, Alarif WM, Algandaby MM, Alburae NA, Alghamdi AM, Nasrullah MZ, Fahmy UA (2021) *Euryops arabicus* us promotes healing of excised wounds in rat skin: Emphasis on its collagen-enhancing, antioxidant, and anti-inflammatory activities. Oxid Med Cell Longev 2021:1–10. https://doi.org/10.1155/2021/8891445
18. Trott O, Olson AJ (2009) AutoDock Vina: Improving the speed and accuracy of docking with a new scoring function, efficient optimization, and multithreading. J Comput Chem 31:455–461. https://doi.org/10.1002/jcc.21334
19. Phillips JC, Braun R, Wang W, Gumbart J, Tajkhorshid E, Villa E, Chipot C, Skeel RD, Kalé L, Schulten K (2005) Scalable molecular dynamics with NAMD. J Comput Chem 26:1781–1802. https://doi.org/10.1002/jcc.20289
20. Jo S, Kim T, Iyer VG, Im W (2008) CHARMM-GUI: a web-based graphical user interface for CHARMM. J Comput Chem 29:1859–1865. https://doi.org/10.1002/jcc
21. Brooks BR, Brooks CL, Mackerell AD, Nilsson L, Petrella RJ, Roux B, Won Y, Archontis G, Bartels C, Boresch S, Caflisch A, Caves L, Cui Q, Dinner AR, Feig M, Fischer S, Gao J, Hodoscek M, Im W, Kuczera K, Lazaridis T, Ma J, Ovchinnikov V, Paci E, Pastor RW, Post CB, Pu JZ, Schaefer M, Tidor B, Venable RM, Woodcock HL, Wu X, Yang W, York DM, Karplus M (2009) CHARMM: the biomolecular simulation program. J Comput Chem 30:1545–1614. https://doi.org/10.1002/jcc.21287
22. Lee J, Cheng X, Swails JM, Yeom MS, Eastman PK, Lemkul JA, Wei S, Buckner J, Jeong JC, Qi Y, Jo S, Pande VS, Case DA, Brooks CL, MacKerell AD, Klauda JB, Im W (2016) CHARMM-GUI input generator for NAMD, GROMACS, AMBER, OpenMM, and CHARMM/OpenMM simulations using the CHARMM36 additive force field. J Chem Theory Comput 12:405–413. https://doi.org/10.1021/acs.jctc.5b00935
23. Halim SA, Sikandari AG, Khan A, Wadood A, Fatmi MQ, Csuk R, Al-Harrasi A (2021) Structure-based virtual screening of tumor necrosis factor-α

inhibitors by cheminformatics approaches and bio-molecular simulation. Biomolecules 11:329. https://doi.org/10.3390/biom11020329
24. Humphrey W, Dalke A, Schulten K (1996) VMD : Visual molecular dynamics. J Mol Graph 14(1):33–38. https://doi.org/10.1016/0263-7855(96)00018-5
25. Holder IA, Boyce ST (1994) Agar well diffusion assay testing of bacterial susceptibility to various antimicrobials in concentrations non-toxic for human cells in culture. Burns 20:426–429. https://doi.org/10.1016/0305-4179(94)90035-3
26. Christensen GD, Baldassarri L, Simpson WA (1995) Methods for studying microbial colonization of plastics. Methods Enzymol 253:477–500
27. Jastaniah SD, Jamal TY, Amashah RH, Aly MM (2022) New strategies for inhibition of Listeria monocytogenes and Klebsiella pneumoniae biofilm formation and persistence. J Contemp Med Sci 8:400–407. https://doi.org/10.22317/jcms.v8i6.1302
28. Elbehairi SEI, Ahmed AE, Alshati AA, Al-Kahtani MA, Alfaifi MY, Alsyaad KM, Alalmie AYA, ElimamAhamed MM, Moustafa MF, Alhag SK, Al-Abd AM, Abbas AM (2020) Prosopis juliflora leave extracts induce cell death of MCF-7, HepG2, and LS-174T cancer cell lines. EXCLI J 19:1282–1294. https://doi.org/10.17179/excli2020-2830
29. Kasibhatla S, Amarante-Mendes GP, Finucane D, Brunner T, Bossy-Wetzel E, Green DR (2006) Acridine orange/ethidium bromide (AO/EB) staining to detect apoptosis. Cold Spring Harb Protoc 2006:4493. https://doi.org/10.1101/pdb.prot4493
30. Hafez S, Jakupovic J, Bohlmann F, Sarg TM, Omar AA (1989) Transformation products of furoeremophilanes and other constituents from *Euryops arabicus*. Phytochemistry 28:843–847. https://doi.org/10.1016/0031-9422(89)80126-8
31. Domínguez DM, Matías R, Villarroel L, Fajardo V, González-Coloma A (2008) Bioactive Furanoeremophilanes from Senecio Otites Kunze Ex DC". Zeitschrift Fur Naturforschung - Section C Journal of Biosciences 63:837–842. https://doi.org/10.1515/znc-2008-11-1209
32. Agulló-Ortuño MT, Díaz CE, González-Coloma A, Reina M (2017) Structure-dependent cytotoxic effects of eremophilanolide sesquiterpenes. Nat Prod Commun 12:663–665. https://doi.org/10.1177/1934578x1701200505
33. Abu-Izneid T, Rauf A, Shariati MA, Khalil AA, Imran M, Rebezov M, Uddin MS, Mahomoodally MF, Rengasamy KRR (2020) Sesquiterpenes and their derivatives-natural anticancer compounds: an update. Pharmacol Res 161:105165. https://doi.org/10.1016/j.phrs.2020.105165
34. Tran KQ, Tin AS, Firestone GL (2014) Artemisinin triggers a G1 cell cycle arrest of human Ishikawa endometrial cancer cells and inhibits cyclin-dependent kinase-4 promoter activity and expression by disrupting nuclear factor-κB transcriptional signaling. Anticancer Drugs 25:270–281. https://doi.org/10.1097/CAD.0000000000000054
35. Tanasova M, Sturla SJ (2012) Chemistry and biology of acylfulvenes: sesquiterpene-derived antitumor agents. Chem Rev 112:3578–3610. https://doi.org/10.1021/cr2001367
36. Fallahian F, Aghaei M, Abdolmohammadi MH, Hamzeloo-Moghadam M (2015) Molecular mechanism of apoptosis induction by Gaillardin, a sesquiterpene lactone, in breast cancer cell lines: Gaillardin-induced apoptosis in breast cancer cell lines. Cell Biol Toxicol 31:295–305. https://doi.org/10.1007/s10565-016-9312-6
37. Rasul A, Khan M, Yu B, Ali M, Bo YJ, Yang H, Ma T (2013) Isoalantolactone, a sesquiterpene lactone, induces apoptosis in SGC-7901 cells via mitochondrial and phosphatidylinositol 3-kinase/Akt signaling pathways. Arch Pharm Res 36:1262–1269. https://doi.org/10.1007/s12272-013-0217-0
38. Rasul A, Yu B, Yang L-F, Arshad M, Khan M, Ma T, Yang H (2012) Costunolide, a sesquiterpene lactone induces G2/M phase arrest and mitochondria-mediated apoptosis in human gastric adenocarcinoma SGC-7901 cells. J Med Plants Res 6:1191–1200. https://doi.org/10.5897/jmpr11.922

Publisher's Note

Springer Nature remains neutral with regard to jurisdictional claims in published maps and institutional affiliations.